International
Progress Report

IPR-04-41

Äspö Hard Rock Laboratory

Äspö Task Force

Modelling of the Tasks 6A, 6B and 6B2 using Posiva streamtube approach

Antti Poteri

VTT Processes

November 2002

Svensk Kärnbränslehantering AB
Swedish Nuclear Fuel
and Waste Management Co
Box 5864
SE-102 40 Stockholm Sweden
Tel 08-459 84 00
+46 8 459 84 00
Fax 08-661 57 19
+46 8 661 57 19

Äspö Hard Rock
Laboratory

Report no.
IPR-04-41
No.
F65K
Author
Antti Poteri
Date
2002-11-01
Checked by
Date
Approved
Christer Svemar
Date
2004-11-23

Äspö Hard Rock Laboratory

Äspö Task Force

Modelling of the Tasks 6A, 6B and 6B2 using Posiva streamtube approach

Antti Poteri

VTT Processes

November 2002

Keywords: Transport modelling, Matrix diffusion, Streamtube approach

Abstract

This report summarises the modelling work of the Tasks 6A, 6B and 6B2. All tasks are modelled using analytical one-dimensional Posiva streamtube approach. This approach assumes that transport takes place through a channel or channels. Processes taken into account in the modelling are advection through the channel(s), sorption on the fracture walls, matrix diffusion to stagnant pools or fault gouge or rock matrix and sorption in the stagnant pool or pore spaces of fault gouge or rock matrix.

Channel geometry defines the flow field and in that way influences the matrix diffusion properties. Channel geometry has been one of the calibration parameters used in Task 6A to fit the model with the measured in-situ tracer test breakthrough curves. In Tasks 6A and 6B a single channel of aperture 2 mm, width 25 mm and length 5.03 m is used. Flow rate and sorption, diffusivity and porosity properties are taken from the data given in the task definition.

Task 6A modelling uses three different immobile pore spaces: stagnant pools, fault gouge and rock matrix. Simulations of the tracer penetration depth in different pore spaces indicate that stagnant pools and fault gouge get saturated in Task 6B conditions. Therefore, Task 6B modelling uses only rock matrix as immobile pore space.

In Task 6B2 transport over larger area of the feature A in considered. Modelling is again based on the streamtube approach. In this case several parallel streamtubes are used. All streamtubes have similar geometry but flow rates vary. The flow rate distribution applied in the Task 6B2 is based on the flow rates measured in five different boreholes using dilution method.

Comparisons of the Task 6B and 6B2 show that if the transport takes place over larger area the breakthrough curves are more spread. Naturally, this comes from the larger spread of the different flow rates (or channels) the tracer encounter in larger region.

Sammanfattning

I denna rapport sammanfattas modelleringsarbetet med Task 6A, 6B och 6B2. I alla tre fallen används Posivas analytiska, endimensionella strömrörsansats. I denna ansats antar man att transporten äger rum i en eller flera kanaler. De processer som man tar hänsyn till i modelleringen är advektion genom kanalerna, sorption på sprickväggarna, matris-diffusion till flödesstagnanta pölar, porutrymmen eller sprickfyllnadsmineral samt sorption i stagnanta pölar och porutrymmen i sprickfyllnadsmineral och bergmatris.

Kanalgeometrin definierar strömningsfältet och därigenom matrisdiffusionsegen-skaperna. Kanalgeometrin har utgjort en av kalibreringsparametrarna som använts i Task 6A för att anpassa modellen till de genombrottskurvor som uppmätts i spårämnesförsök in-situ. I Task 6A och 6B har en enskild spricka med vidden 2 mm, bredden 25 mm och längden 5.03 m använts. För flöde, sorption, diffusivitet och porositet har de data som angivits i arbetsdefinitionen använts.

I Task 6A-modelleringen används tre olika immobila porutrymmen: stagnanta pölar, sprickfyllnadsmineral och bergmatrisen. Simuleringar av spårämnenas penetrationsdjup i de olika porutrymmena antyder att de stagnanta pölarna och sprickfyllnadsmineralen mättas upp under de förhållanden som antas i Task 6B. I Task 6B2 genomförs beräkningarna för en större yta inom Feature A. Återigen baseras modelleringen på strömrörsansatsen. I detta fall används flera parallella strömrör. Alla strömrören har samma geometri men flödet varierar mellan strömrören. Den använda statistiska fördelningen av flödet bygger på flödesmätningar i fem borrhål med utspädningsmetoden.

En jämförelse mellan 6B och 6B2 visar at genombrottskurvorna blir mer utspridda om transporten äger rum över en större yta. Detta härrör naturligtvis från att spårämnena känner av en större spridning av flödeshastigheten i ett större område.

Executive Summary

Task 6 is a modelling task of the Äspö Force on Modelling of Groundwater Flow and Transport of Solutes. Task 6 is an exercise to link site characterisation and performance assessment approaches to solute transport.

This report summarises modelling of the Tasks 6A, 6B and 6B2. Task 6A revisits the TRUE-1 tracer test STT-1b. This tracer test was performed in single feature between two packed-off borehole sections. Distance between the injection and extraction borehole sections was 5.03 m. Tracer test was performed using several tracers from non-sorbing to weakly and moderately sorbing tracers. Task 6A is modelled for four different tracers: iodine, strontium, cobalt, technetium and americium. All but americium were also used in the STT-1b test. In Task 6B the same flow path is used as in Task 6A and using the same tracers but the flow rate is reduced by a factor 1000. Task 6B2 is an extension of the Task 6B where the source and sink are changed to allow transport over wider area of the tested hydraulic feature.

The modelling approach presented in this report is based on the application of the performance assessment type model on both in-situ tracer tests and to the extrapolation of the transport processes into the temporal scale of the performance assessment. Modelling of all tasks is based on the streamtube approach. This means that flow path is represented by a collection of streamlines.

In the radial converging test the source area is small, i.e. the injection borehole. In this case a single transport channel is assumed to make up the flow path. In Task 6B2 the source is 2 m wide line source and several parallel transport channels are developed.

Simulation of the transport in Task 6A and 6B show that the retardation in the scale of the in-situ tracer experiments and in the scale of the performance may be dominated by different geological units. Tracer experiment scale can take advantage of the rather small capacity pore spaces like fault gouge and stagnant. This kind of small capacity pore space is also the potential altered rim zone of the rock matrix next to the fracture. However, the effect of the altered rim zone has not been analysed in the present modelling.

Due to the large difference in the pore diffusivity and porosity between the rock matrix and small capacity pore spaces it seems also possible that the retarding influence of the matrix diffusion is smaller in the performance assessment scale (as it is defined in this exercise) than in the in-situ tracer experiment scale.

In the Task 6B2 the transport takes place over larger area of the feature A. Task 6B2 modelling is based on the available flow measurements in the feature A. The flow rates are measured in five boreholes, which intersect the feature A. Naturally, this gives quite coarse picture of the flow rate distribution. This can be seen as peaky tracer discharge in the modelling results. Especially the retention due to the matrix diffusion is quite sensitive to the flow rate and this further enhances the differences in the retention potential of the different transport channels. This is reflected in the modelling results as wider spread of the breakthrough curve. First breakthrough takes place earlier than in the Task 6B and tailing is also longer.

Contents

1 Introduction

Task 6 is a modelling exercise that tries to link the site characterisation and performance assessment approach to solute transport in fractured rock. The focus of the Task 6 is in the 50-100 m scale that is considered critical for the performance assessment in the present repository programs.

The approach in Task 6 is to apply both site characterisation and performance assessment models for same tracer experiments. Conditions relevant for the performance assessment are derived from the experimental set-up by changing the boundary conditions.

According to the Task 6 modelling task specification the characteristics of the Task 6 are:

- Task 6 combines the use of PA and SC models for both PA and SC boundary conditions.
- All modellers should first implement their models such that they can reproduce the results from relevant Äspö in situ tracer experiments.
- Modellers can make appropriate assumptions for PA modelling, while continuing to honour the in situ tracer experiment result.

Task 6 is composed of six subtasks that are:

Task 6A: Model and reproduce selected TRUE-1 tests with a PA model and/or a SC model.

Task 6B: Model selected PA cases at the TRUE-1 site with new PA relevant (long term/base case) boundary conditions and temporal scales.

Task 6B2: An extension of the Task 6B where boundary conditions are modified to produce flow and transport over a larger area of the feature tested in Task 6A.

Task 6C: Develop a 50-100m block scale synthesised structural model using data from the Prototype Repository, TRUE Block Scale, TRUE-1 and FCC.

Task 6D: This task is similar to Task 6A, using the synthetic structural model and a 50 to 100 m scale TRUE-Block Scale tracer experiment.

Task 6E: Task 6E extends the Task 6D transport calculations to a reference set of PA time scales and boundary conditions.

This report summarises the modelling work of the Tasks 6A, 6B and 6B2.

2 Objectives

According to the task definition the objectives of Task 6 are to:

1. Assess simplifications used in PA models.
2. Assess the constraining power of tracer (and flow) experiments for PA models.
3. Provide input for site characterisation programs from a PA perspective (i.e., provide support for site characterisation program design and execution aimed at delivering needed data for PA).
4. Understand the site-specific flow and transport behaviour at different scales using SC models.

The modelling approach described in this report is based on performance assessment type

3 Task 6A and Task 6B

3.1 Task 6A definition

In Task 6A transport takes place in a single hydraulic feature through a relatively short flow path (about 5 meters). Task 6A is based on the TRUE-1 tracer test STT-1b that was performed in a single hydraulically isolated feature, called feature A. The tracer test was performed between two packed-off borehole sections. The flow field was radial converging and no over-pressure was applied in the injection borehole. Figure 1 illustrates the experimental configuration, positions of the boreholes and the expected flow path.

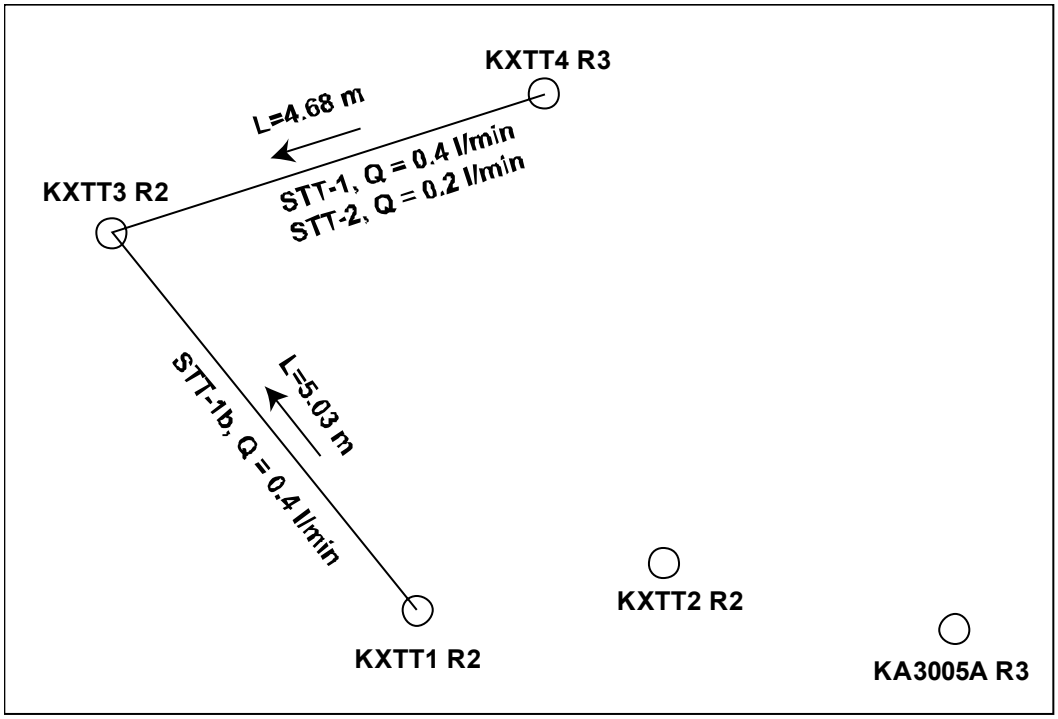

Figure 1. *Illustration of the experimental set-up of the TRUE-1 sorbing tracer experiments (from Selroos and Elert, 2001). Task 6A and 6B are based on the configuration of the STT-1b experiment.*

Selroos and Elert (2001) present the detailed definition of the Tasks 6A and 6B. According to the task definition transport of iodine, strontium, cobalt, technetium and americium are to be modelled along the STT-1b flow path in the feature A at the TRUE-1 site. Feature A is believed to be a reactivated mylonite that has been exposed to brittle deformation. It is interpreted to be bounded by a rim zone of higher porosity consisting of altered Äspö diorite, which constitutes a band of disturbed rock along the studied feature. The total thickness of the feature including altered Äspö diorite is varying between 0.05 and 0.09 m and the physical aperture of the fracture is estimated to be in the order of 1-3 mm.

The distance in the STT-1b test between the injection and withdrawal boreholes was 5.03 m. The tracer experiment was carried out by injecting a finite pulse tracer pulse of 4 hours. The pumping in the withdrawal section was 0.4 l/min. The flow rate in the injection section was estimated to be 41.9 ml/h at 0 – 4 hours and 58.1 ml/h at 20 – 151 hours. STT-1b test did not include americium and technetium as tracers but the injection time histories of americium and technetium are assumed to be identical to that of Co-60.

Selroos and Elert (2001) give also the sorption and diffusivity data for the elements modelled in the Task 6A. This data is presented in Table 1.

Table 1. Sorption and diffusivity data for additional tracers (from Selroos and Elert, 2001).

Tracer	Kd (m^3/kg)	Ka (m)	De (m^2/s)
I	0	0	$8.3\ 10^{-14}$
Co	0.0008	0.008	$2.9\ 10^{-14}$
Tc	0.2	0.2	$4\ 10^{-14}$
Am	0.5	0.5	$4\ 10^{-14}$

Simulations are requested both for the measured injection functions and for a Dirac pulse injection. Radioactive decay should not be considered in the modelling and simulations should be performed up to time of 10 years or a full recovery.

Requested performance measures of the Task 6A are:

- Drawdown in the injection and pumping borehole (if available)
- Breakthrough time history for each tracer.
- Maximum release rate (Bq/a)
- The breakthrough times for the recovery of 5, 50 and 95 % of the injected mass: t5, t50 and t95.

3.2 Task 6B definition

Task 6B is basically Task 6A but using lower flow rates. Transport is expected take place along the same fracture and between the same borehole sections as in the Task 6A. Conditions of the Task 6A are transformed to the conditions relevant for the performance assessment by assuming that the flow rate is 1000 times lower in Task 6B as in Task 6A. It is also stated that the background head field observed during TRUE-1 experiment is not applicable in Task 6B because the tunnel is not expected to influence the flow field in Task 6B.

Two types of tracer injection function are applied in Task 6B: a constant injection of 1 MBq/year and a Dirac pulse injection. Radioactive decay is not taken into account in this task and simulations are requested to be performed up to a time of 10^6 years or until full recovery.

Performance measures of the Task 6B include breakthrough time history for each tracer and maximum release rate. In addition, for the Dirac pulse injection also breakthrough times for the recovery of 5, 50 and 95% of the injected mass are required.

3.3 Modelling approach

Modelling is based on the streamtube approach in which a single flow channel describes the flow path. The modelling takes into account three main processes: advection, matrix diffusion and sorption both on the fracture walls and in the matrix. Sorption, pore diffusivity and porosity properties are taken from the data given in the task definition. Geometry of the channel is modified to calibrate the modelled breakthrough against the measured outcome of the STT-1b test.

Matrix diffusion can take place to different geological units containing immobile pore space. Three different immobile pore spaces are considered: stagnant pools of the flow field, fault gouge and rock matrix. Basis of the model calibration has been the measured breakthrough curves of I-131, Sr-85 and Co-60 in the STT-1b test.

It should be noted that the single channel model gives always eventually 100% recovery. STT-1b test does not show 100% recovery for all tracers. Partly, this follows from the limited monitoring time in the extraction borehole. However, if the ultimate recovery is extrapolated based on the observed breakthrough curves then full recovery is not reached for all tracers. Extrapolation shows ultimate recoveries of 100% for iodine, 87% for strontium and 44% for cobalt. Modelling of Task 6A does not try to resolve what have caused the low recoveries but it only takes it as experimental observation that need to be taken into account when the channel model is calibrated with the measured breakthrough curves.

Applied modelling approach is based on analytical solution of the tracer transport through the flow channel. In addition to the analytical transport model the penetration depth of the matrix diffusion is estimated by applying Monte-Carlo simulations.

3.3.1 Transport model

The tracer discharge for a Dirac pulse injection is calculated using Equation (1).

$$\frac{\dot{m}}{m_0} = j(t, t_w, u, R_a) = H(t - R_a t_w) \frac{u}{\sqrt{\pi}(t - R_a t_w)^{3/2}} e^{-\frac{u^2}{t - R_a t_w}}, \qquad (1)$$

where H denotes Heviside's step function, t_w is the groundwater transit time, R_a is the retardation factor of the surface sorption and parameter group u determines the strength of the matrix diffusion. Parameter group u is defined in Equation (2).

$$u = \frac{D_e x}{v\ 2b}\sqrt{\frac{R_p}{D_p}} = \sqrt{D_e \varepsilon R_p}\,\frac{t_w}{2b} = \sqrt{D_e \varepsilon R_p}\,\frac{W x}{Q}, \qquad (2)$$

where D_e is the effective diffusion coefficient in the matrix, v is the groundwater flow velocity, $2b$ is the fracture aperture, D_p is the pore diffusivity in the matrix, R_p is the retardation coefficient in the matrix, ε is the porosity of the matrix, W is the width of the flow channel, x is the length of the flow channel and Q is the flow rate through the flow channel.

3.3.2 Transport channel

Transport channel is simplified to a rectangular tube. Length of the tube is taken from the distance between the injection and extraction borehole sections along the tested feature. This gives length of 5.03 m. The volume of the channel follows from the fitting of the non-sorbing HTO breakthrough curve and assuming a plug flow through the transport channel. The HTO fitting gave groundwater transit time of t_w = 4.34 hours in Task 6A. The flow velocity and parameter group u value was used to fit the breakthrough curves. Following the definition of the Task 6B the groundwater transit time t_w = 4 340 hours in Task 6B.

It is assumed that the immobile pore spaces are located as indicated in Figure 2. Stagnant water may be available in the fracture plane i.e. to the lateral direction through the side walls of the transport channel, fault gouge is assumed to be distributed in the flow channel as small particles and rock matrix is available through the ceiling and floor of the channel. In this way each matrix diffusion process can be conveniently parametrised. Channel width is connected to the coupling with matrix diffusion to the rock matrix, aperture is coupled to the matrix diffusion to the stagnant zones and finally matrix diffusion to the fault gouge is characterised by "generalised aperture" that is connected to the average distance between fault gouge particles. Altered rim zone of the rock matrix is not taken into account in the modelling.

One constraint for the channel geometry is that the flow rate through it is known. From injection curve it is derived that the flow rate through the injection borehole section have been approximately 58 ml/h (Selroos and Elert, 2001). The cross-sectional area of the channel, the flow rate and groundwater transit time should be consistent. This, together with the constraining power of the measured breakthrough curves gives following channel geometry: aperture 2 mm, width 25 mm and length 5.03 m.

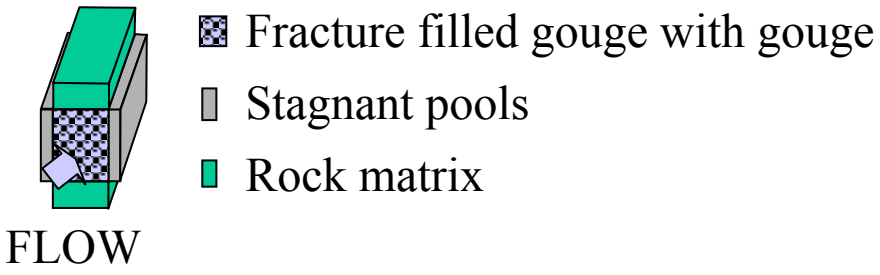

Figure 2. *Conceptualisation of the immobile pore spaces and transport channel. See text for detailed explanation.*

3.3.3 Tracer penetration depth to the immobile pore space

Penetration depth of the matrix diffusion is estimated by applying Monte-Carlo simulations of the advection-matrix diffusion process. The approach is to model the diffusion process to the matrix by one dimensional random walk sequence using fixed length of the time step. It is noted that the advective part of the transport process can be simplified to a counter that calculates the time tracer molecule spends in the advective pore space. This simplification is based on the assumption that there is a good

(diffusional) mixing over the fracture aperture. In practice this means that for an ideal non-sorbing tracer (without matrix diffusion) there will be only one transit time through the transport channel (i.e. like plug flow). This means also that when a tracer molecule has spent the transit time, t_w, in the mobile part it has gone through flow channel. In this way the Monte-Carlo simulation of the advection-matrix diffusion process can be reduced to a one-dimensional diffusion process conditioned by the molecules residence time in the mobile pore space. This is illustrated in Figure 3.

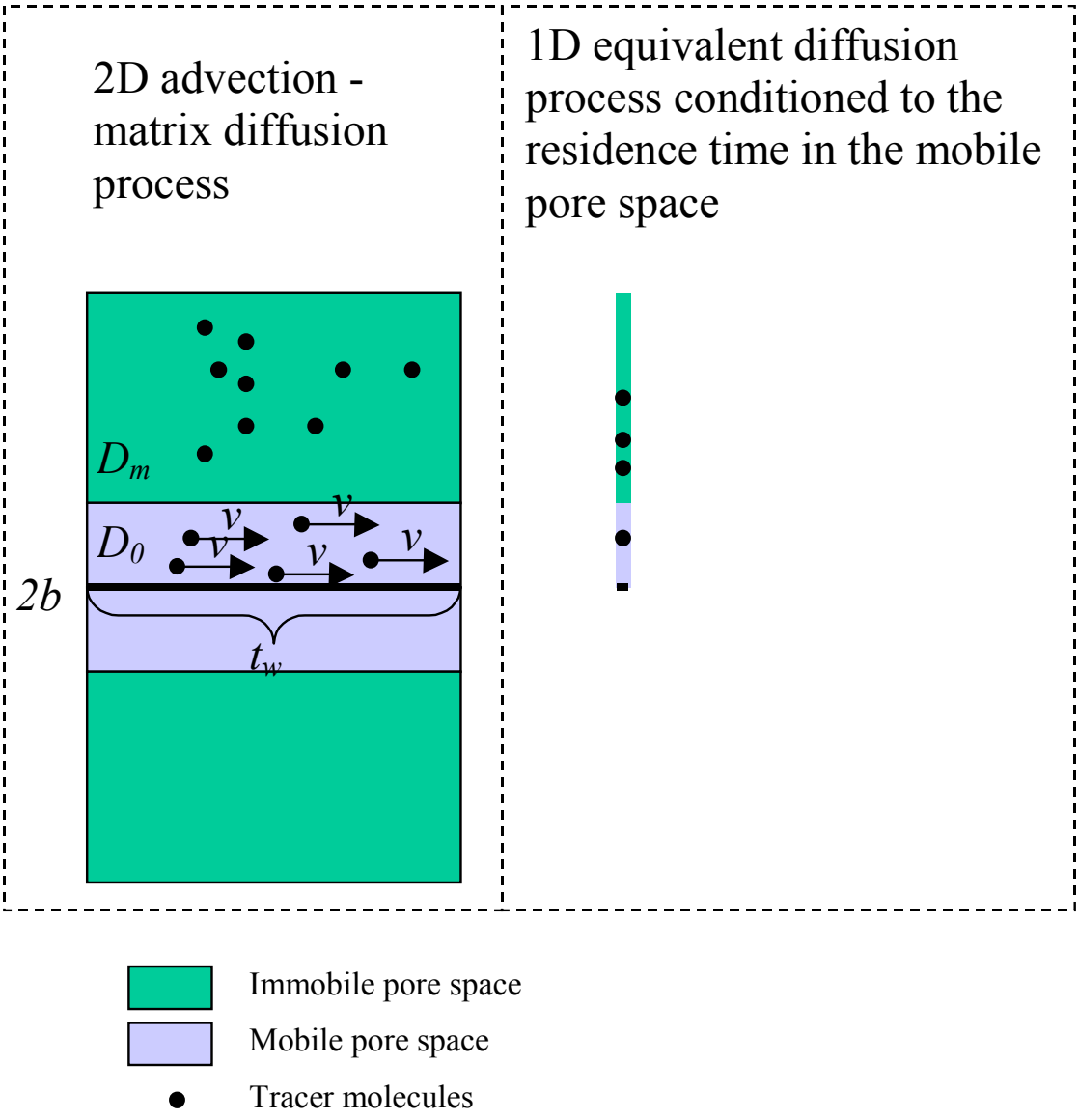

Figure 3. *Schematic illustration how the advection – matrix diffusion can be reduced to a one-dimensional diffusion process that is conditioned to the residence time in the mobile pore space.*

The one-dimensional Monte-Carlo simulation technique was tested using large matrix thickness that behaves like infinite matrix during the tested time interval. Results of the Monte-Carlo simulation were compared with the corresponding analytical solution. According to the comparison the Monte-Carlo simulation method is an excellent agreement with the analytical solution (see Figure 4).

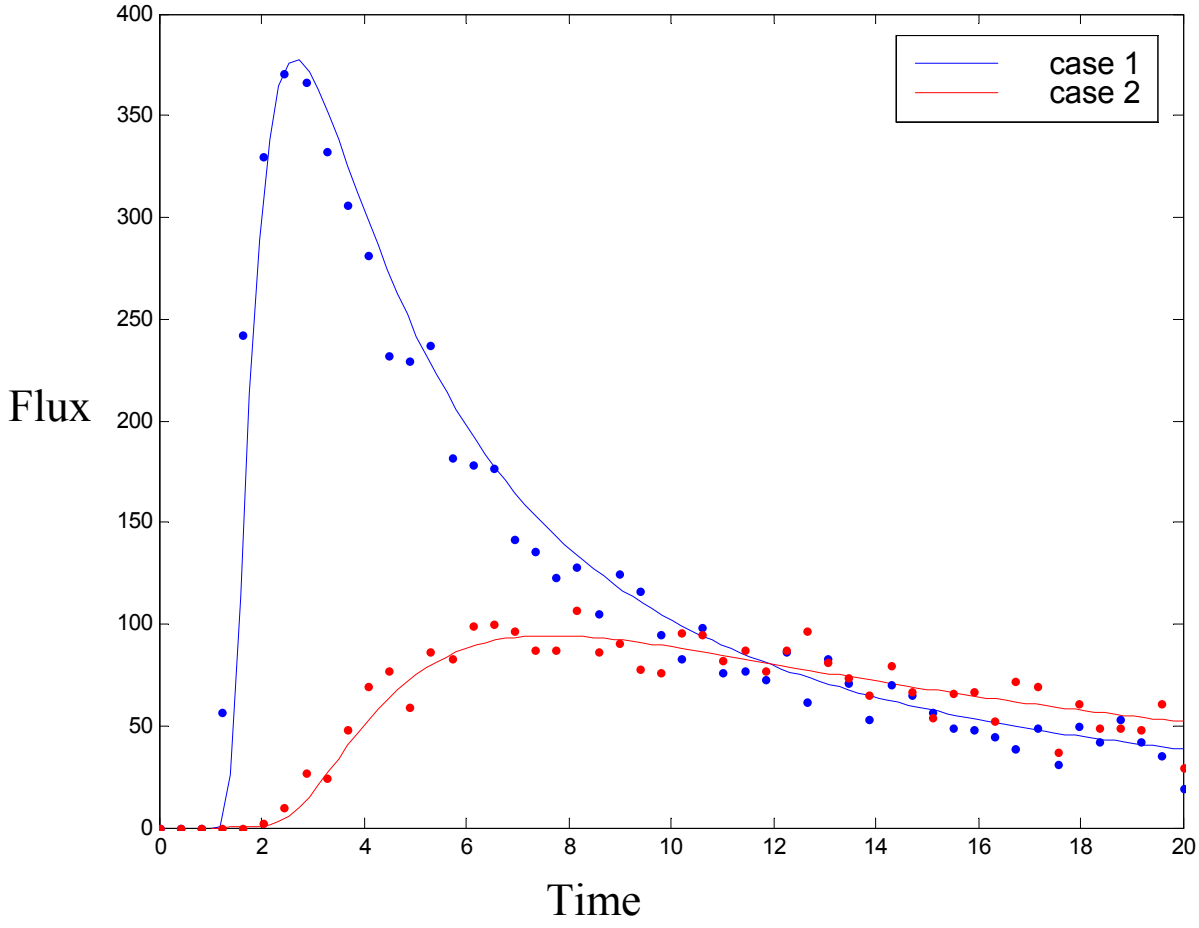

Figure 4. *Monte-Carlo simulations (dots) and analytical solution of the breakthrough curves for the advection – matrix diffusion in the case of infinite matrix.*

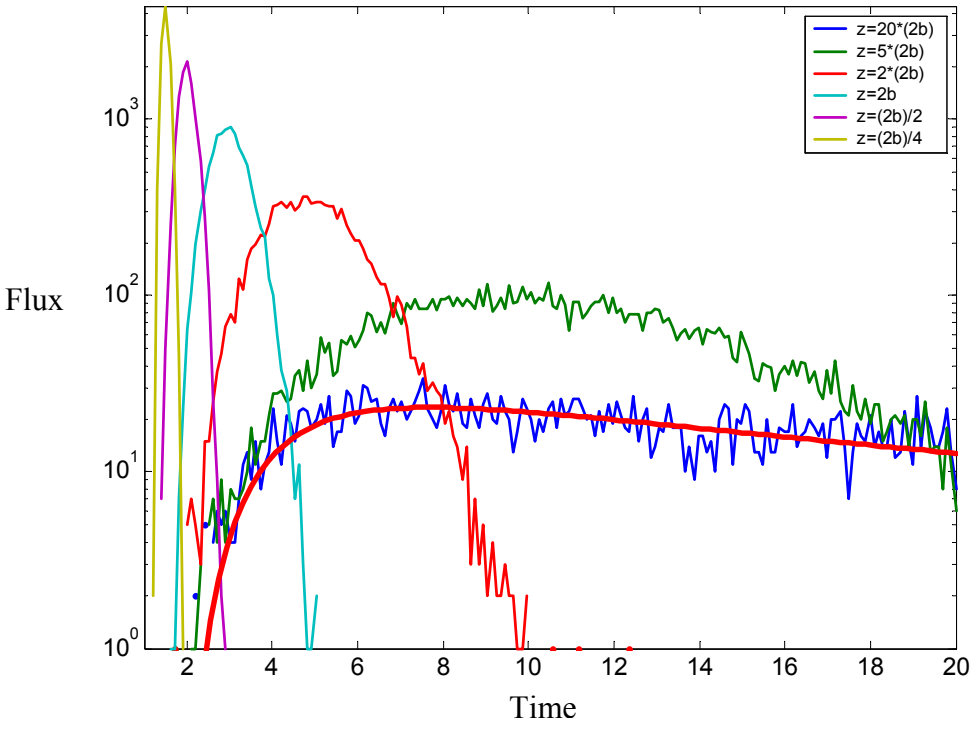

Figure 5. *Monte-Carlo simulation of the breakthrough curve for varied matrix thickness. In figure 2b is the fracture aperture, so matrix thickness varies from 0.25*aperture to 20*aperture. Groundwater transit time is one time unit. Thick red line is the analytical solution for an infinite matrix thickness.*

Penetration depth of the tracers into immobile zones was simulated at the same time for both the Task 6A and 6B conditions. Simulations were carried out for non-sorbing tracer and termination time of the simulation was 10 times the groundwater transit time. It is clear that tracer particles coming out at the late time in the tailing of the breakthrough have also had chance to visit the greatest depth in the immobile pore space. In this modelling exercise it was considered sufficient to apply termination time of 10 times the groundwater transit time. The maximum penetration depths are presented for all particles whether they had passed the whole transport channel or not.

Distribution of the maximum penetration depths of the 500 particles simulated is presented in Figure 6. Based on the simulation it is evident that during the Task 6B flow conditions the stagnant zones and fault gouge get saturated. For this reason the Task 6B simulation is based only on the sorption on the fracture walls, matrix diffusion to the rock matrix and sorption in the rock matrix. Task 6A simulation is based on the same sorption processes but matrix diffusion is possible to the stagnant zones, fault gouge and rock matrix. In the Task 6B the fault gouge and stagnant zones contribute to the equilibrium sorption (surface sorption) but this effect is not taken into account in the modelling.

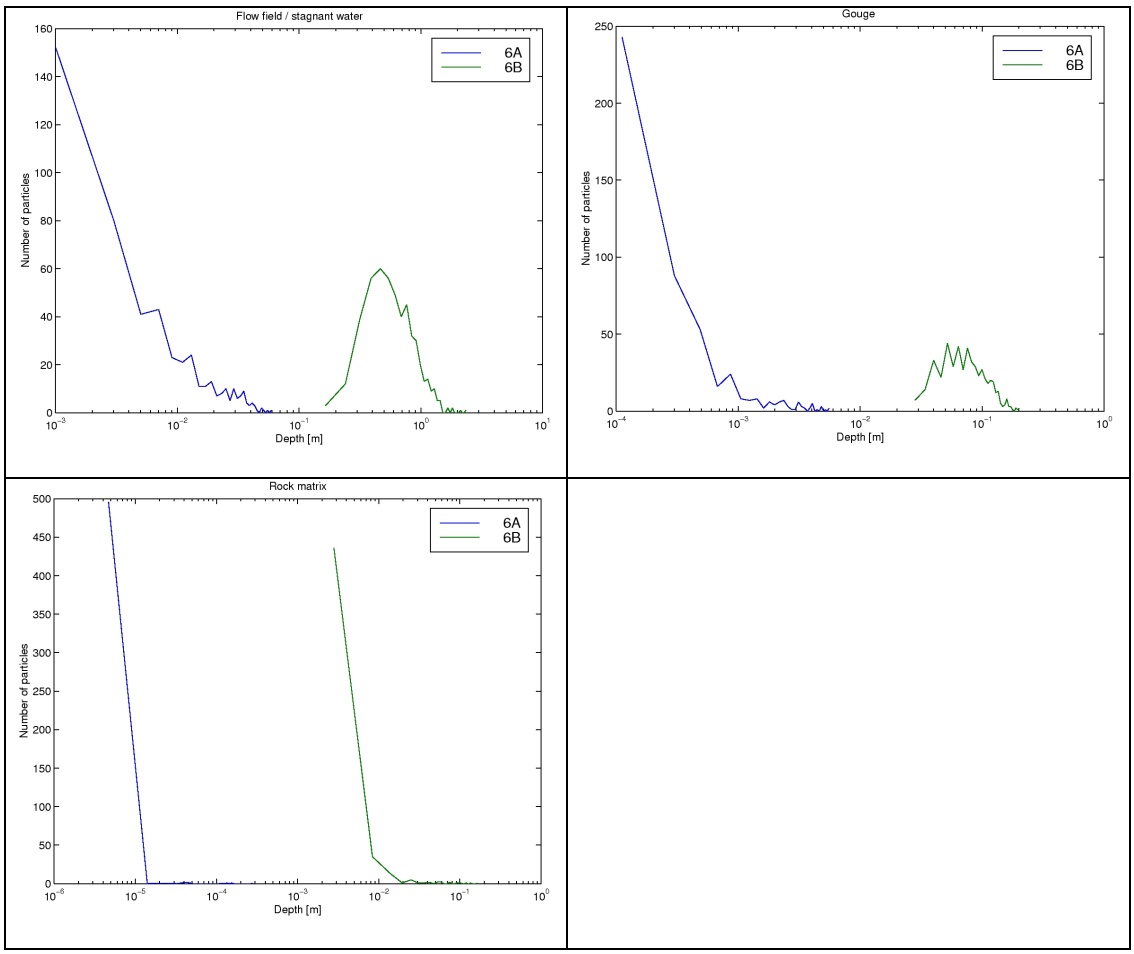

3.3.4 Transport parameters

Transport parameters in the Task 6A and 6B were determined by estimating the importance of different geological units (stagnant pools, fault gouge and rock matrix) for the retardation. Basically, the sorption and porosity parameters were taken from Selroos and Elert (2001). The analytical transport model assumes infinite thickness of the immobile zone. This means that if the immobile zone is expected to get saturated it is simply not included in the matrix diffusion model. The saturated immobile zone causes retardation that is similar to the equilibrium sorption. However, in these cases the surface sorption term (R_a) has not been enhanced by the aforementioned mechanism.

Stagnant pools are assumed to be regions in the fracture's void space where the flow is extremely slow or completely stagnant. Because the stagnant pools are assumed to be in the fracture the sorption is described by surface sorption.

Matrix diffusion to different geological units is examined using following approach. If we look at the matrix diffusion solution (1) more in detail we observe that

$$j(t,t_w,u,R_a) = \frac{j(t/R_a,t_w,u/\sqrt{R_a},1)}{R_a} \quad . \tag{3}$$

Let the breakthrough curve of the tracer without surface sorption (i.e. R_a=1) be

$$k(t) = \int_0^t j(t,t_w,u,1)b(t_w)dt_w \quad , \tag{4}$$

where $b(t_w)$ is the groundwater transit time distribution. Similarly a tracer with surface sorption gives breakthrough curve that is

$$k'(t) = \int_0^t j(t,t_w,u*,R_a)b(t_w)dt_w \quad . \tag{5}$$

Equation (3) indicates now that $k'(t)$ can be scaled to $k(t)$ by R_a if $u = u*/\sqrt{R_a}$.

This offers us a way to compare matrix diffusion properties of the tracers that have different surface sorption properties. To compare the tracers we need to take away the periods of time when the tracer molecule is sorbed on the fracture wall and concentrate only on the periods when the tracer is available for the matrix diffusion. In practice this nothing but scaling the breakthrough curves by the surface retardation coefficient. For the measured tracers we do not know the R_a's. However, this does not complicate the comparison too much: we simply take all the tracers measured for the same flow path and scale the first arrival time to be same for all breakthrough curves. This is based on the assumption that first arrival time is (mainly) governed by the equilibrium sorption and groundwater transit time distribution.

What we observe is the spreading of the scaled breakthrough curves. Let us assume that one of our tracers is non-sorbing. Scaling other tracers' first breakthrough at the same time point as the non-sorbing tracer should give the R_a of that tracer. The width of the scaled breakthrough (i.e. tracer with R_a) is narrower than the non-sorbing breakthrough

if the retardation factor in matrix, R_p, is smaller than R_a and it is broader if the $R_p > R_a$. In the special case that $R_p = R_a$ the scaled sorbing and non-sorbing breakthrough curves should coincide. These conclusions hold if it is assumed that the other parameters in u (D_e, ε, W, x and Q, see Equation (2)) are same for all tracers. A questionable assumption is here connected to the D_e (or D_p) that to some extent depends on tracer.

This approach is not suitable if there are large differences in the retardation between the breakthrough curves. For a strongly sorbing tracer the groundwater transit time is not at all important in determining the breakthrough curve. This makes the scaling based on the first breakthrough time completely useless and leads certainly wrong conclusions. However, in the case of STT-1b test the tracers are only moderately sorbing. Iodine, strontium and cobalt breakthrough curves can be scaled to the same first arrival time by using scaling factors of 9 or smaller. In this case it regarded that there is still reasonable dependence between the retardation and groundwater transit time so that trendsetting observation can be made.

One should also note that R_a is not completely independent of u as here is assumed. Especially, for strongly sorbing tracers R_a depends linearly on the flow field dependent part of the u (i.e. WL/Q or $t_w/2b$). If we consider single velocity channel and short injection we can write for the time of the maximum discharge in the case of equilibrium sorption

$$t_{\max} = \left(1 + \frac{2}{2b} K_a\right) t_w = t_w + 2K_a \frac{t_w}{2b} = t_w + 2K_a \frac{WL}{Q} \quad . \qquad 6$$

Similarly in case of the diffusion to the immobile zone we get

$$t_{\max} = t_w + \frac{2}{3} u^2 = t_w + \frac{2}{3} D_e \varepsilon R_p \left(\frac{WL}{Q}\right)^2 \quad . \qquad 7$$

This means that if the same flow path is tested using different flow rates the observed breakthrough time as a function of the flow rate should turn from linear behaviour to quadratic behaviour when the diffusion to the stagnant zones begins to dominate the retention. In practice this should show the behaviour that the calculated retardation coefficient is constant as long as the equilibrium sorption dominates but begins to increase when the diffusion process dominates.

Measured breakthrough curves of the STT-1b test that are scaled to the same first breakthrough time are presented in Figure 7. Both cobalt and strontium breakthrough curves indicate that Rp > Ra. If the matrix diffusion takes place only to the stagnant pools that have approximately the same aperture than fracture (i.e. the stagnant pools are in the fracture) then should be Rp ≈ Ra. Thus, Figure 7 indicate that the measured breakthrough curves cannot be explained by the matrix diffusion to the stagnant pools only. For this reason also matrix diffusion to the fault is considered. Alternatively, altered zone at the surface of the rock matrix may cause the same effect, but this is not considered in this model.

Modelling of the Task 6A is based on the surface sorption on the fracture walls and matrix diffusion to stagnant pools, fault gouge and rock matrix. In the case of Task 6B the simulations of the penetration depth of the non-sorbing tracer indicate that stagnant pools and fault gouge get saturated. For this reason the Task 6B modelling is based only on the matrix diffusion to the rock matrix and surface sorption. The possible enhancement of the surface sorption caused by the saturated stagnant pools and fault gouge is not taken into account.

The retention parameters of the Task 6A and 6B are based on the data given by Selroos and Elert (2001). K_d's and K_a's for the fault gouge are basically same as for the rock matrix except that the K_d's for the cobalt and strontium are increased by a factor of 10. In Tables 2, 3 and 4 are presented the sorption parameters for the stagnant water, fault gouge and rock matrix, respectively.

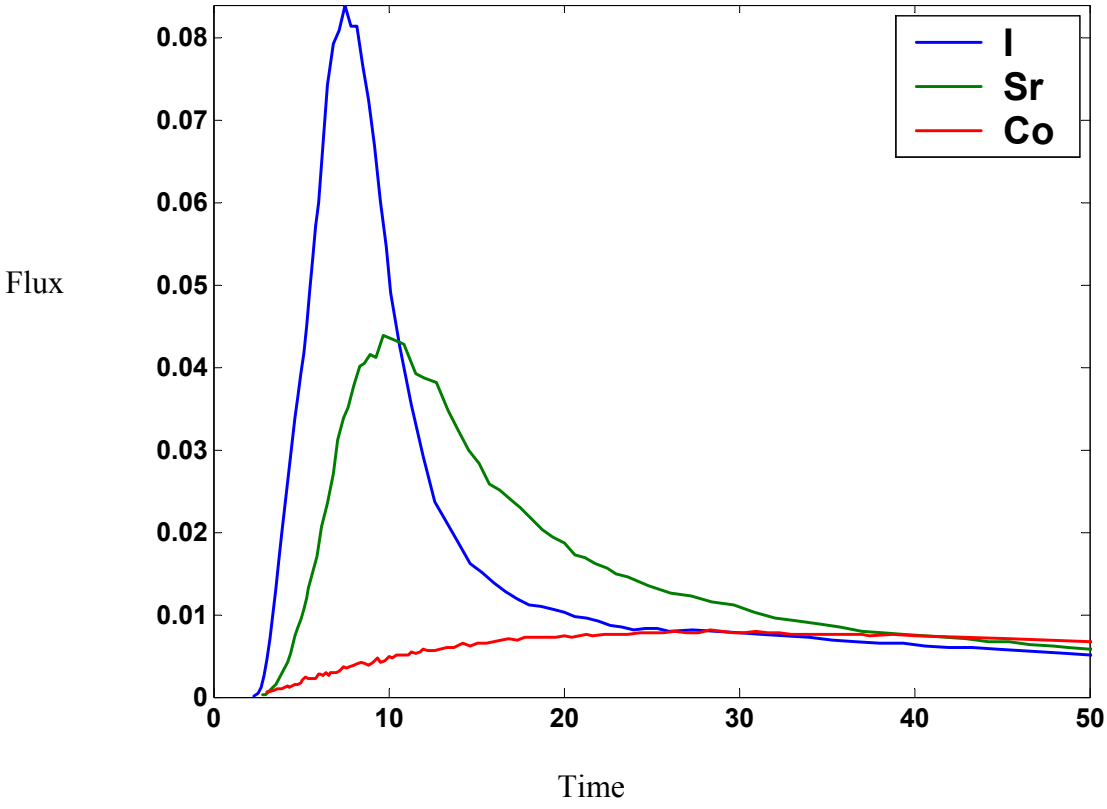

Figure 7. *Scaled measured breakthrough curves for iodine, strontium and cobalt. All curves are scaled to have the same first breakthrough time.*

Table 2. Sorption parameters for the stagnant pools. K_a values are taken from Selroos and Elert (2001).

	K_a	2b [m]	R_a
I	0	2.00E-03	1
Sr	8.00E-06	2.00E-03	1.008
Co	0.008	2.00E-03	9
Tc	0.2	2.00E-03	201
Am	0.5	2.00E-03	501

Table 3. Sorption parameters for the fault gouge. Kd and Ka are rock matrix sorption properties taken from Selroos and Elert (2001), except cobalt and strontium that are given ten times the rock matrix Kd's.

	K_a	K_d	Poros.	Density [kg/m3]	2b [m]	R_a	R_p
I	0	0	0.03	2630	2.00E-03	1	1
Sr	8E-06	4.7E-05	0.03	2630	2.00E-03	1.008	5
Co	0.008	0.008	0.03	2630	2.00E-03	9	681
Tc	0.2	0.2	0.03	2630	2.00E-03	201	17005
Am	0.5	0.5	0.03	2630	2.00E-03	501	42512

Table 4. Sorption parameters for the rock matrix. K_d's are taken from Selroos and Elert (2001).

	K_a	K_d	Density [kg/m3]	Poros.	2b [m]	R_a	R_p
I	0	0	2700	0.004	2.00E-03	1	1
Sr	8E-06	4.7.E-06	2700	0.004	2.00E-03	1.008	4.16
Co	0.008	0.0008	2700	0.004	2.00E-03	9	539
Tc	0.2	0.2	2700	0.004	2.00E-03	201	134461
Am	0.5	0.5	2700	0.004	2.00E-03	501	336151

Retention parameter applied in the modelling is the parameter group *u* introduced in (2). In Task 6A stagnant pools, fault gouge and rock matrix are available for the matrix diffusion at the same time. It means that Task 6A model parameter *u* is sum of the stagnant pool *u*, fault gouge *u* and rock matrix *u*. In Task 6B model parameter *u* is only the rock matrix *u*. In Table 5 are presented the *u*-values for Task 6A and Task 6B. In addition to the sorption parameters also flow channel or flow field properties are needed (cf. Equation (2)). These are presented in Section 3.3.2 and they are a result of the fitting of the STT-1b breakthrough curves. Groundwater transit times are 4.34 h and 4 340 h for the Task 6A and Task 6B, respectively. The parameter group *u* presented in Table 5 includes also a "generalised" aperture measure. For stagnant pools it is the effective (or average) width of the channel because stagnant pools are assumed to exist in the lateral direction to the flow channel in the fracture plane. For rock matrix it is the effective aperture of the channel because rock matrix is assumed to exist in the perpendicular direction to the fracture plane. For the fault gouge it is a "generalised" aperture that correlates with the density of the fault gouge particles that are assumed to fill the flow channel.

Table 5. Matrix diffusion parameters for Task 6A and Task 6B.

	Task 6A				Task 6B
	u **stagnant [sqrt(h)]**	***u*** **gouge [sqrt(h)]**	***u*** **rock [sqrt(h)]**	**u total [sqrt(h)]**	***u*** **rock [sqrt(h)]**
I-131	0.51	0.54	0.0029	1.05	2.89
Sr-85	0.51	1.21	0.0059	1.73	5.90
Co-60	1.53	14.14	0.067	15.74	67.10
Tc-99m	7.23	70.67	1.06	78.96	1059.91
Am-241	11.41	111.74	1.68	124.83	1675.85

3.4 Task 6A results

Breakthrough curves of the Task 6A modelling are presented in Figures 8 to 12. For iodine, strontium and cobalt also the measured STT-1b test breakthrough curves are presented. Table 6 presents the performance measures of the Task 6A.

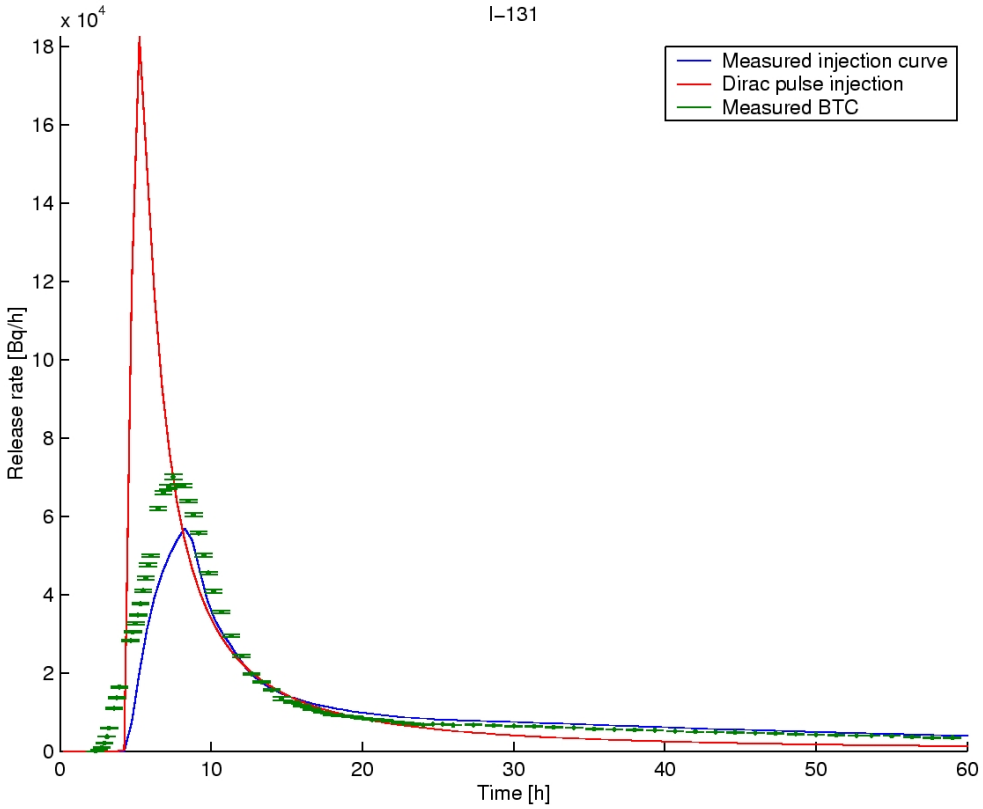

Figure 8. *Simulated and measured breakthrough curves for iodine.*

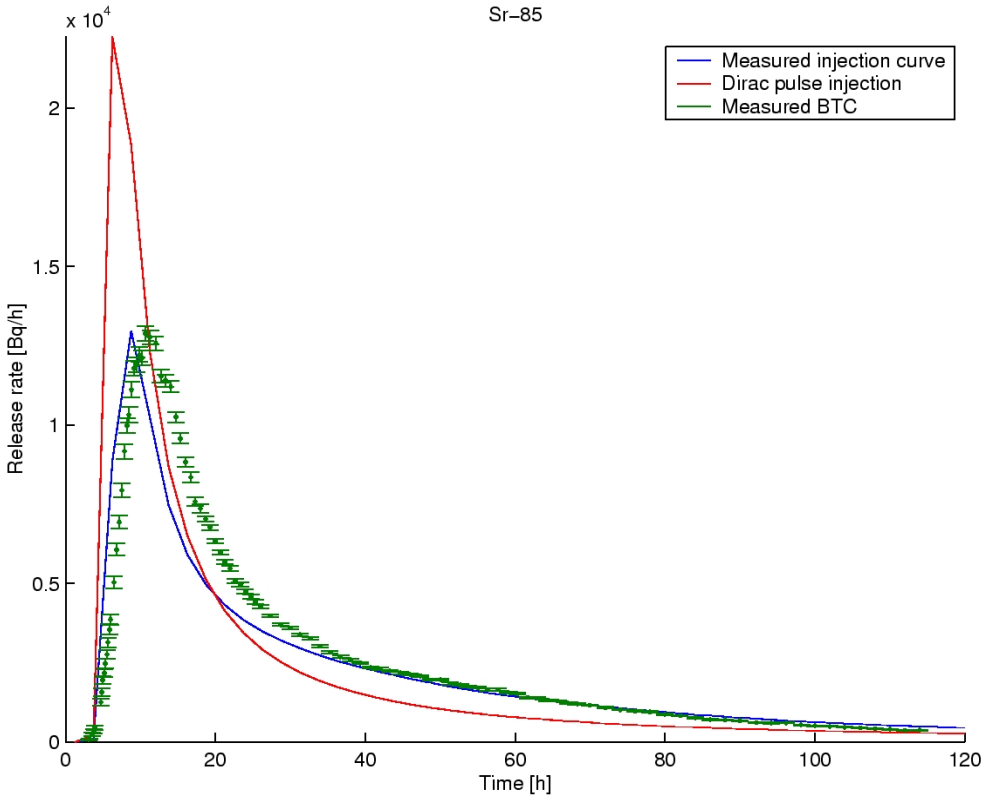

Figure 9. *Simulated and measured breakthrough curves for strontium.*

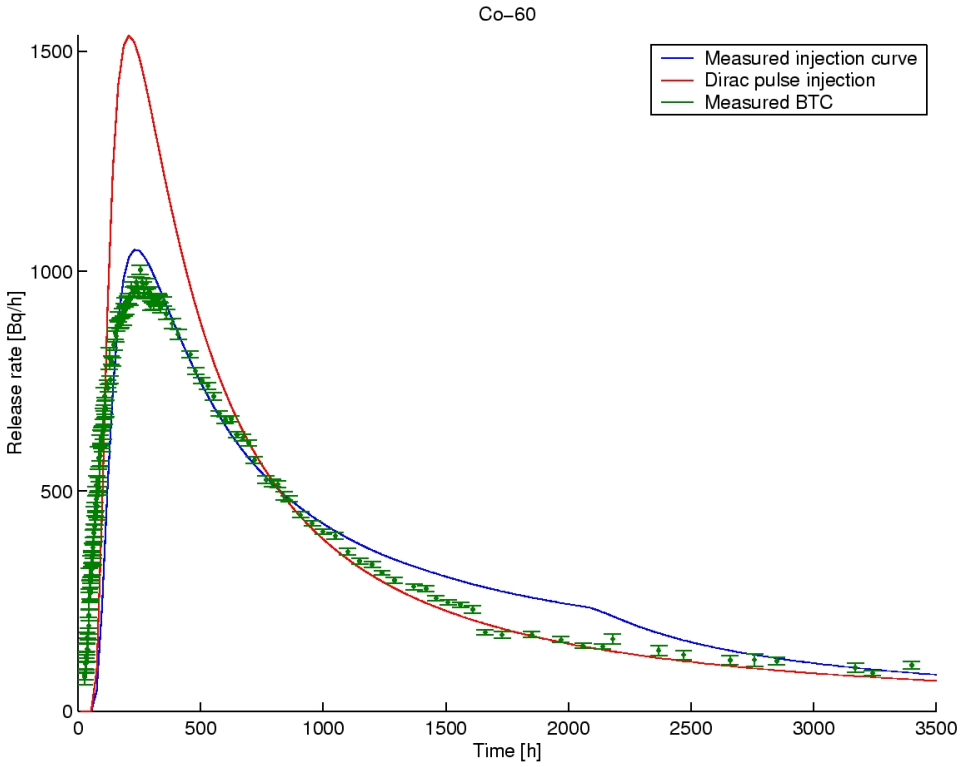

Figure 10. *Simulated and measured breakthrough curves for cobalt.*

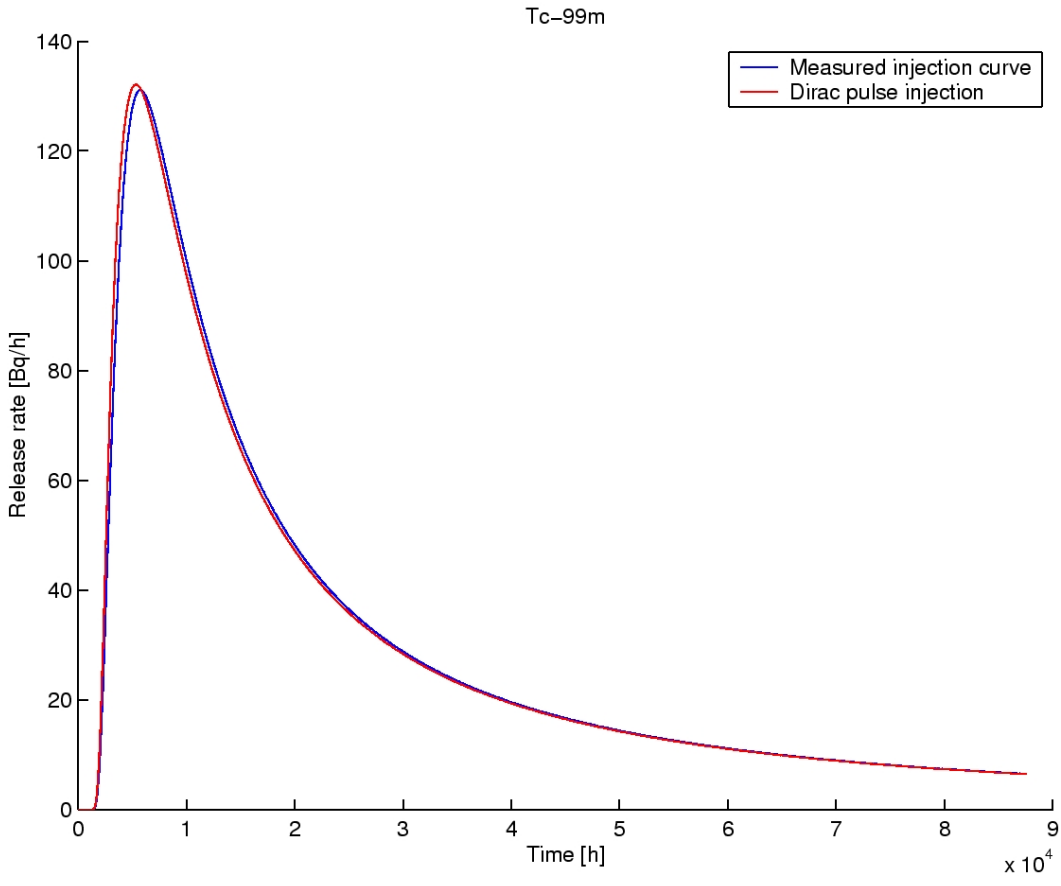

Figure 11*. Simulated breakthrough curves for technetium.*

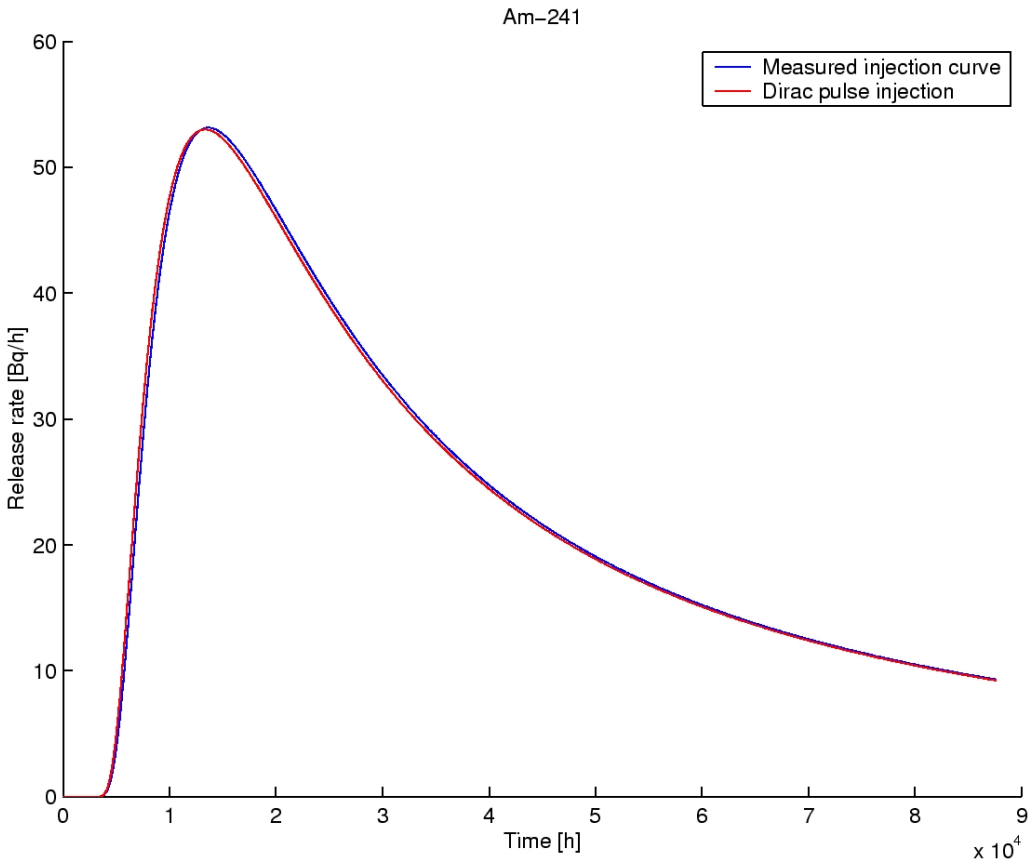

Figure 12. *Simulated and measured breakthrough curves for americium.*

Table 6. Performance measures for the Task 6A.

	Maximum release rate [Bq/a]	
	Dirac injection	**Measured injection**
I-131	21.7	6.5
Sr-85	3	1.5
Co-60	0.18	0.12
Tc-99m	0.015	0.015
Am-241	0.0061	0.0061

	Breakthrough times [a]		
	t 5%	**t 50%**	**t 95%**
I-131, Dirac inj.	0.00056	0.0011	0.066
Meas. inj.	0.00077	0.0033	0.053
Sr-85, Dirac inj.	0.00068	0.0020	0.18
Meas. inj.	0.0010	0.0039	0.12
Co-60, Dirac inj.	0.020	0.13	15
Meas. inj.	0.024	0.18	>10
Tc-99m, Dirac inj.	0.50	3.47	390
Meas. inj.	0.53	3.47	>10
Am-241, Dirac inj.	1.24	8.65	972
Meas. inj.	1.27	8.60	>10

3.5 Task 6B results

Breakthrough curves of the Task 6B modelling are presented in Figure 13 and 14 and the performance measures are presented in Table 7.

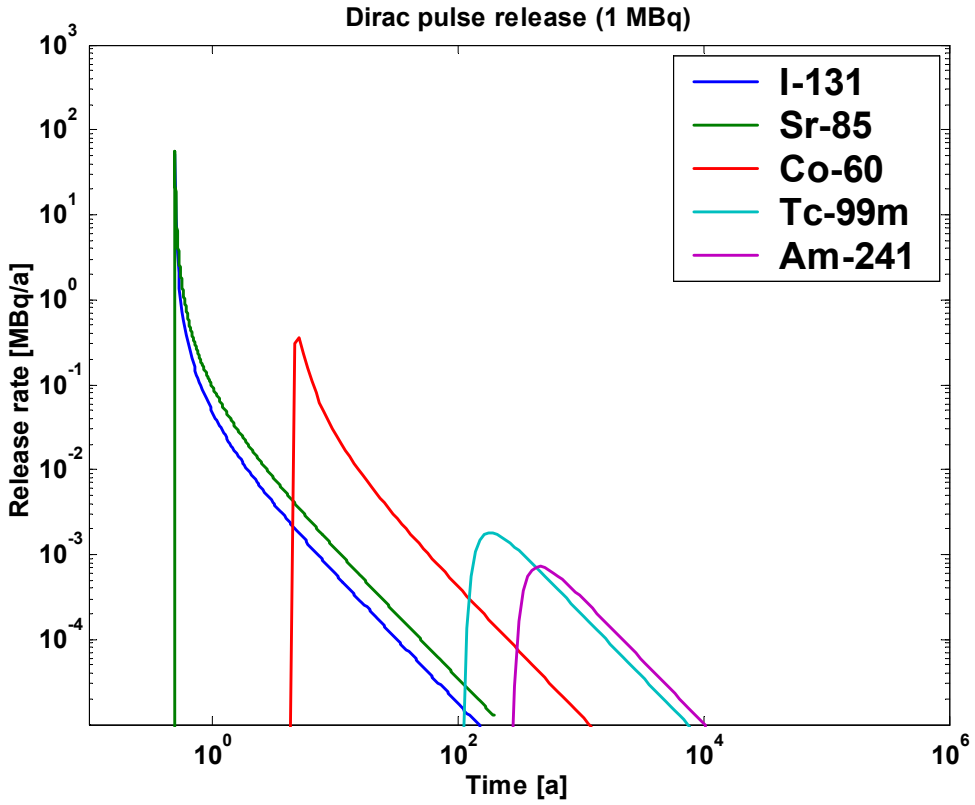

Figure 13. *Task 6B breakthrough curves for the Dirac injection function.*

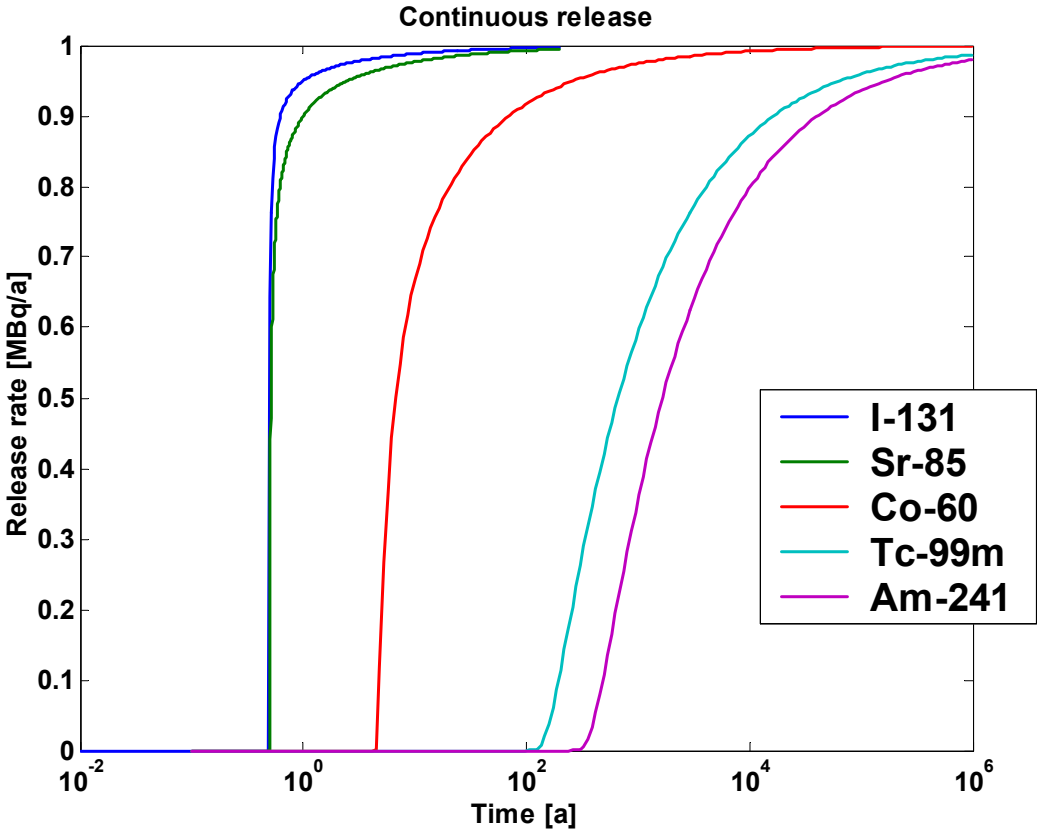

Figure 14. *Task 6B breakthrough curves for the continuous injection function.*

Table 7. Performance measures of the Task 6B.

	Maximum release rate [MBq/a]	
	Dirac injection	**Continuous injection**
I-131	231	1.00
Sr-85	58	1.00
Co-60	0.45	1.00
Tc-99m	0.0018	0.99
Am-241	0.00072	0.98

	Breakthrough times [a]		
	t 5%	**t 50%**	**t 95%**
I-131, Dirac	0.50	0.50	1.0
Sr-85, Dirac	0.50	0.51	2.5
Co-60, Dirac	4.7	6.7	267
Tc-99m, Dirac	166	664	65 349
Am-241, Dirac	415	1654	162 880

4 Task 6B2

4.1 Task definition

Elert and Selroos (2001) give task 6B2 definition. According to the task definition Task 6B2 is an extension of the Task 6B. In Task 6B source area is the injection borehole section of the STT-1b test. In Task 6B2 the source area is extended to have transport over larger area of the feature investigated in the TRUE-1 experiments. The concept is illustrated in Figure 15. Flow field is governed by two fractures intersecting the feature A, which was tested in the STT-1b test. Constant hydraulic heads are applied to the intersecting fractures to give 0.1% hydraulic gradient over the feature A.

The injection is made over a 2 meters line source, which is parallel to the intersecting fractures and is centred at the borehole section KXTT1:R2. Tracer is collected at fracture Y that is located at ten meters distance from the source.

The same tracers as in Tasks 6A and 6B are modelled, i.e. iodine, strontium, cobalt, technetium and americium. Two types of tracer injection boundary condition are used: a constant injection of 1 MBq/year and a Dirac pulse input (unit input).

Performance measures of the Task 6B2 include for both the constant injection rate and the Dirac pulse injection the breakthrough time history for each tracer. In addition, for the Dirac pulse injection the performance measures include the maximum release rate (1/a) and the breakthrough times for the recovery of 5, 50 and 95 % of the injected mass (in years).

As in the Tasks 6A and 6B radioactive decay is not taken into account in Task 6B2.

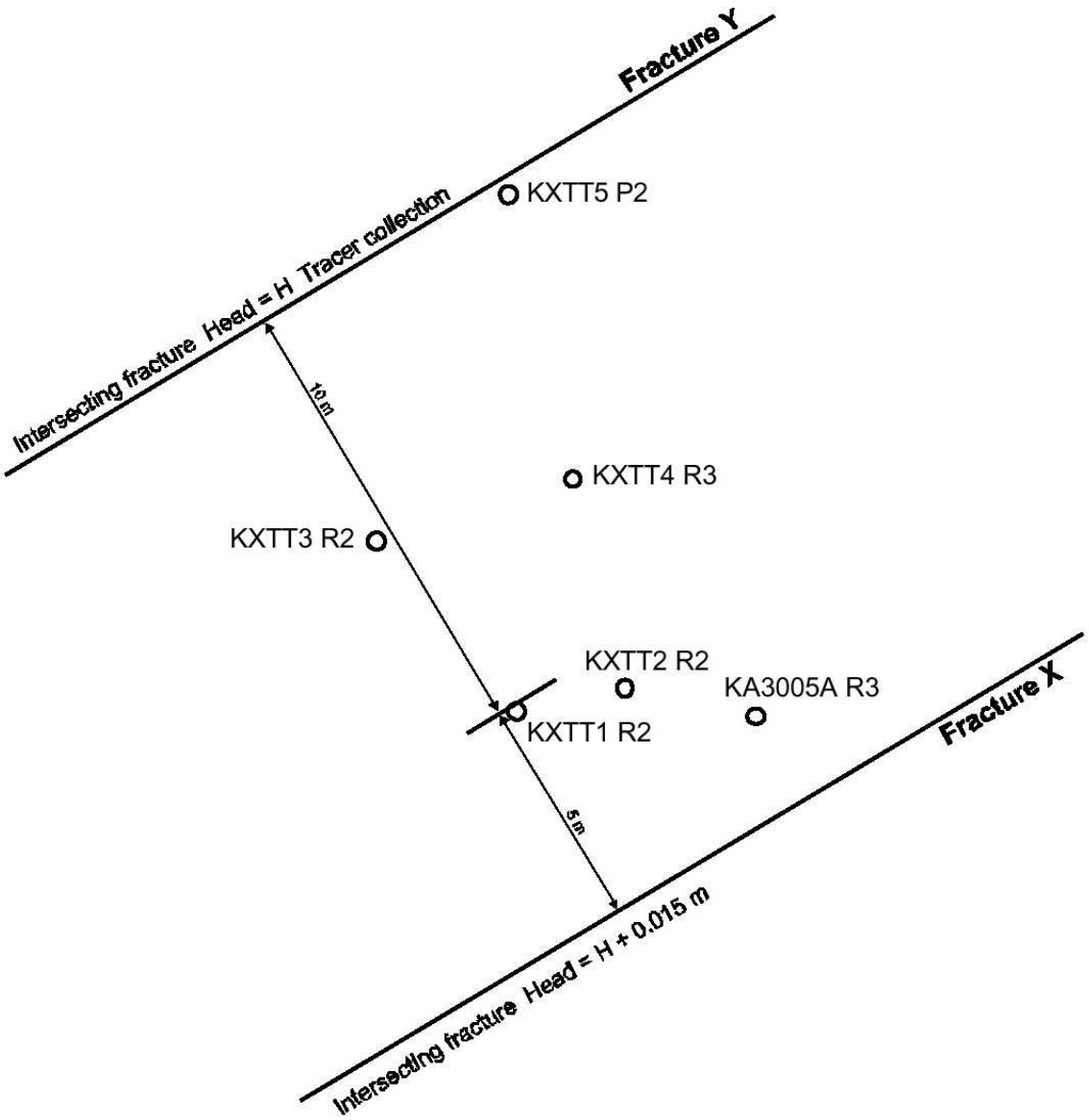

Figure 15. *Geometry of the Task 6B2 (from Elert and Selroos, 2001).*

4.2 Modelling approach

Modelling of the Task 6B2 is based on the one-dimensional analytical (Posiva streamtube) approach similarly as Tasks 6A and 6B. Processes that are taken into account are advection, sorption and matrix diffusion to the rock matrix. Based on the experience from the Task 6B stagnant zones and fault gouge are assumed to be saturated by the tracers. As in the Task 6B the saturated fault gouge or stagnant pools are not taken into account as an enhanced surface sorption term.

In Task 6B the transport channel was the same as in the STT-1b and for that reason the flow rate through the transport channel was known. In Task 6B2 this is not the case, because transport may take place through several parallel channels on feature A and these channels are not tested in any tracer test. Modelling of the Task 6B2 need to be based on the statistical description of the potential flow paths.

4.2.1 Transport model

Transport of the tracers is modelled by assuming several parallel transport channels between the source and sink. Assuming plug flow (good mixing of the tracer during transport through the channel) we can write that the transit time through i[th] channel is $t_w = WL(2b)/Q_i$. Breakthrough curve of the unit Dirac input to N channel system is then

$$\dot{m} = \sum_{i=1}^{N} \frac{u_i}{\sqrt{\pi}\sqrt{\left(t-(2b+2K_a)\frac{WL}{Q_i}\right)^3}} \exp\left(-\frac{u_i^{\,2}}{t-(2b+2K_a)\frac{WL}{Q_i}}\right). \quad (8)$$

This shows that we need to know the distribution of the flow rate through the N channel system. It is assumed that the flow field through the 2 m wide line source to the sink is statistically similar to the flow field at any region of the feature A. If we are able to estimate the flow rates at different positions in feature A, then the same statistics should also hold for the simulated flow paths.

Equation (8) shows also two additional assumptions that have been made in the representation of the flow rate distribution. The flow rates are given for fixed width (W) and all channels have the same length (L). It is noted here that the width (W) in the transport model is the width that the tracer molecules see in the flow field. The width W is estimated when the flow rate distribution is known.

4.2.2 Distribution of the flow in the feature A

Distribution of the flow over the feature A can be simulated for the given boundary condition if the statistics and spatial structure of the transmissivity over feature A is known. There is not very much information on the spatial structure of the transmissivity on feature A. Therefore, a more straightforward approach is applied. First, it is noted that a set of flow rate measurements has been performed in feature A under "undisturbed" flow conditions. The "undisturbed" flow conditions means here a flow field without pumping in the feature A, of course the presence of the tunnel may have strong influence on these measured flow rates.

Head measurements that were made simultaneously with the dilution flow measurements show rather constant gradient of the hydraulic head field over the feature A during the dilution tests (see Figure 16). This gives opportunity to use directly the measured distribution dilution flow rates and scale them by the ratio between the defined hydraulic gradient in Task 6B (0.1%) and the measured hydraulic gradients of the corresponding dilution measurements. Fitting of the constant gradient to the heads measured in the dilution test #2 gives approximately 7% gradient of the hydraulic head during the dilution measurement.

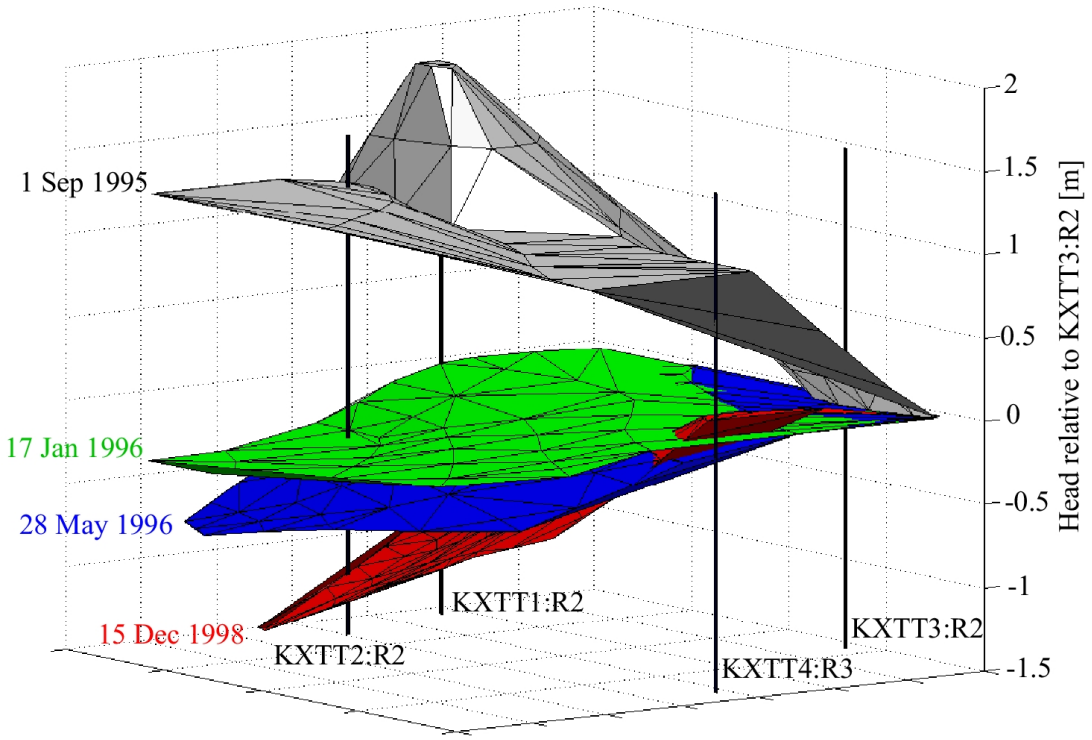

Figure 16. *Head field in feature A during different dilution tests. Head fields are presented relative to the head in the borehole section KXTT3:R2. Head fields are composed from Andersson et al (1997) and Winberg et al (1998).*

The dilution measurements represent flow rate that is approximately over the diameter of the borehole. Here it is assumed that the dilution measurement gives flow rate over 10 cm wide region. Flow rates are taken from the dilution test #2 (Andersson and Wass, 1997). In that test flow rates were measured in all five boreholes in feature A. The measured flow rates are given in Table 8. This table includes also scaled flow rates that correspond to the flow conditions of the Task 6B2.

Table 8. Measured flow rates in the dilution test #2 and corresponding flow rates that are scaled into Task 6B2 flow conditions.

Borehole	Dilution test #2 conditions April, 1997 (grad(h) ~ 7%) [ml/min]	Task 6B2 conditions (grad(h) = 0.1%) [litres/a]
KXTT1	0.08	0.60
KXTT2	0.01	0.075
KXTT3	1.67	12.5
KXTT4	0.01	0.075
KA3005A	0.18	1.4

Flow rates in Table 8 are used to simulate the flow rate distribution of the flow parallel channels that intersect the 2 m line source. The scaled flow rates in Table 8 are assumed to represent the flow rates over a 10 cm scale that is a little bit larger than the diameter of the borehole. The 2 m line source is divided into 10 cm intervals and flow rates for the intervals are sampled from the flow rates in Table 8.

As noted in the Section 4.2.1 the width seen by the tracer molecules needs to be known for the transport calculations. This is done by simulating the advection and transverse diffusion through the simulated flow field of the parallel flow channels intersecting the 2 m line source. The same 2 mm channel aperture is used as in the Task 6A and 6B and the path lengths are fixed to 10 m. A set of 10 000 particles were released randomly over the 2 m line source and the width they scan during the transport was recorded. The distribution of the widths is presented in Figure 17. The distribution is quite wide and to simplify the modelling the transport calculations are based on the average width of 20 cm.

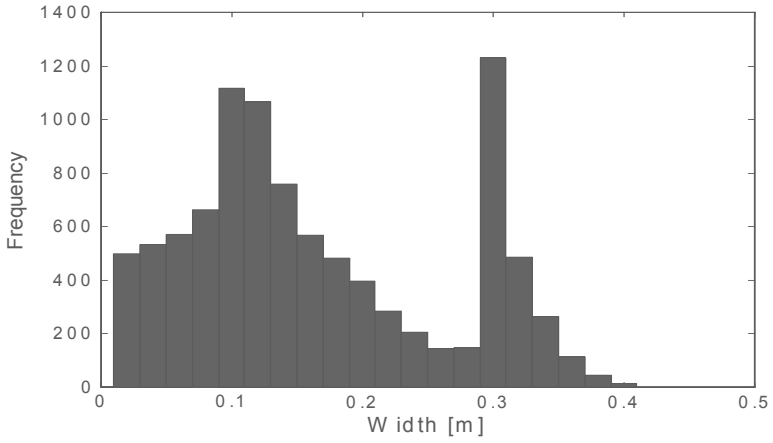

Figure 17. *Distribution of the transverse width scanned by the tracer molecules in the advective field.*

4.2.3 Transport simulations

The same sorption data as in the Task 6B has been used. It is also assumed, as in the Task 6B, that matrix diffusion takes place only to the rock matrix. The reasoning of this is based on the simulations of the Task 6B that show saturation of the other immobile pore spaces that were considered in Task 6A. It is true that the flow field in Task 6B2 is not exactly similar to the Task 6B flow channel, but the simulations showed tracer penetration depths in Task 6B that extend to decimetre scale. Based on this it is concluded that other pore spaces than rock matrix will very likely saturate also in Task 6B2.

Sorption parameters used for the transport simulation are presented in Table 9.

Tracer transport is simulated using a set of 100 000 tracer particles. The procedure applied for the transport simulations is following:

1. Width of the transport channel (i.e. width seen by the tracer molecules) is set to 0.2 m
2. Using measured dilution flow rates a random composition of parallel flow channels is build using the five measured flow rates. Widths of the channels are 0.1 m, which is assumed to be the measurement scale in dilution tests.
3. Introduce a tracer particle at random position in the system of five parallel channels and integrate how much flow is over 0.2 m width that is on average seen by the tracer.
4. Calculate the tracer discharge using Equation (8) and W=0.2 m, L=10 m, and Q as calculated in step 3. Other parameters according to Table 9.

Table 9. Parameters used in the transport simulation of the Task 6B2.

	Ka [m]	Kd [kg/m3]	Rock density [kg/m3]	Rock porosity	De [m2/a]
I	0	0	2700	0.004	2.6E-06
Sr	8.00.E-06	4.70.E-06	2700	0.004	1.3E-06
Co	0.008	0.0008	2700	0.004	9.1E-07
Tc	0.2	0.2	2700	0.004	1.3E-06
Am	0.5	0.5	2700	0.004	1.3E-06

Path width	0.2 m (The width that is seen by the tracer molecules)
Path length	10 m
Aperture	2 mm
Porosity	0.004
Rock density	2700 kg/m3

4.3 Results

The simulations are based on the measured flow rates at five different points in feature A. This gives quite rough description of the possible flow rates through transport channels. In the transport simulations the flow rates are further averaged over width of two flow channels, but still the results show the characteristics of the rough flow rate distribution. This can be seen as rugged and peaky discharge especially in Figure 18.

Performance measures of the Task 6B2 are presented in Table 110.

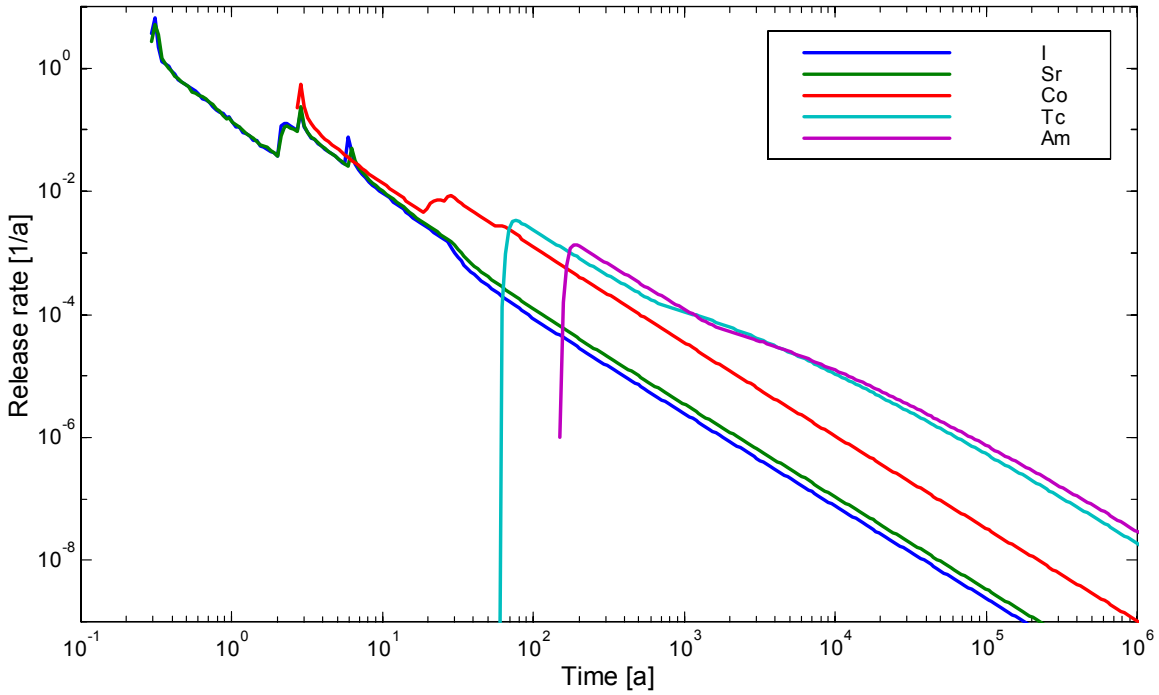

Figure 18. *Tracer discharge in Task 6B2, Dirac input.*

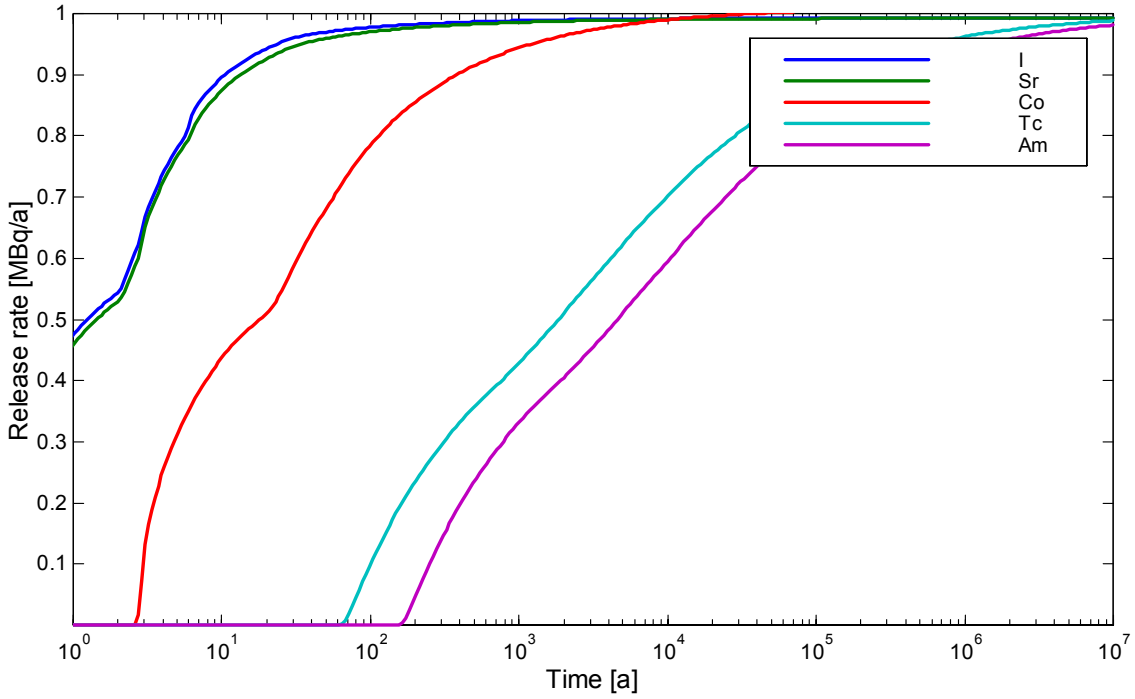

Figure 19. *Tracer discharge in Task 6B2, continuous release on 1 MBq/a.*

Table 10. Performance measures of the Task 6B2.

Tracer	t 5 % [a]	t 50 % [a]	t 95% [a]	Max release rate [1/a]
I-131	0.3	1	20	7.0
Sr-85	0.3	1	30	5.0
Co-60	3	20	1 000	0.6
Tc-99m	80	2 000	600 000	0.003
Am-241	200	5 000	1 000 000	0.001

5 Discussion

Simulation of the transport in Task 6A and 6B show that the retardation in the scale of the in-situ tracer experiments and in the scale of the performance may be dominated by different geological units. Tracer experiment scale can take advantage of the rather small capacity pore spaces like fault gouge and stagnant. This kind of small capacity pore space is also the potential altered rim zone of the rock matrix next to the fracture. However, the effect of the altered rim zone has not been analysed in the present modelling.

Due to the large difference in the pore diffusivity and porosity between the rock matrix and small capacity pore spaces it seems also possible that the retarding influence of the matrix diffusion is smaller in the performance assessment scale (as it is defined in this exercise) than in the in-situ tracer experiment scale.

In the Task 6B2 the transport takes place over larger area of the feature A. Task 6B2 modelling is based on the available flow measurements in the feature A. The flow rates are measured in five boreholes, which intersect the feature A. Naturally, this gives quite coarse picture of the flow rate distribution. This can be seen as peaky tracer discharge in the modelling results. Especially the retention due to the matrix diffusion is quite sensitive to the flow rate and this further enhances the differences in the retention potential of the different transport channels. This is reflected in the modelling results as wider spread of the breakthrough curve. First breakthrough takes place earlier than in the Task 6B and tailing is also longer.

6 References

Andersson, P. and Wass, E., 1997. TRUE 1st stage tracer test programme. Dilution tests, run # 2, March-April 1997. Äspö Hard Rock Laboratory, Technical Note, TN-97-26t. SKB, Sweden, 1997.

Andersson, P., Nordqvist, R. and Jönsson, S., 1997. Äspö Hard Rock Laboratory, TRUE 1st stage tracer test programme. Experimental data and preliminary evaluation of the TRUE-1 dipole tracer tests DP-1 – DP-4. SKB Progress Report HRL-97-13.

Benabderrahmane, H., Dershowitz, W., Selroos, J.-O., Uchida, M., and Winberg, A., 2000. Task 6: Performance Assessment Modelling Using Site Characterisation Data (PASC). November 28, 2000.

Elert, M. and Selroos, J.-O., 2001. Task 6B2 Modelling task specification, version 1.0. December 7, 2001.

Selroos, J.-O., Elert, M., 2001. Task 6A & 6B Modelling task specification, Version 1.0. April 3, 2001.

Winberg, A., Andersson, P., Hermanson, J. and Byegård, J., 1998. First TRUE stage. Updated structural model of the TRUE-1 Block and detailed description of feature A. A technical memorandum prepared for the Äspö Task Force, Tasks 4E/4F. December 1998.